Brillouin scattering study of molten zinc chloride

C. Dreyfus,* M. J. Lebon, F. Vivicorsi, A. Aouadi, and R. M. Pick
LMDH, Université Pierre et Marie Curie, 4 Place Jussieu, 75252 Paris Cedex 05, France

H. Z. Cummins
Physics Department, City College of the City University of New York, New York, New York 10031
(Received 4 August 2000; published 29 March 2001)

Polarized and depolarized Brillouin scattering experiments on molten $ZnCl_2$ were performed between 300 and 600 °C in different geometries. VV spectra measured in backscattering and small angle scattering were analyzed with conventional viscoelastic theory using either a Debye or a Cole-Davidson model for the memory function. We also analyzed in the same way the temperature dependence of the transverse Brillouin lines detected in a 90° VH geometry. We show that the Cole-Davidson memory function yields a consistent interpretation of all the spectra. The resulting shear and longitudinal relaxation times are equal within their error bars, and are about 2.5 times smaller than the α relaxation time previously determined. The static shear viscosity values deduced from the analysis of the propagating transverse waves agree, at all temperatures, with the measured viscosity values.

DOI: 10.1103/PhysRevE.63.041509 PACS number(s): 64.70.Pf, 66.20.+d, 78.35.+c

I. INTRODUCTION

The viscoelastic behavior of supercooled liquids has been investigated using different techniques for many years. Nevertheless, neither the details of the slow relaxation process observed in all materials showing a liquid-glass transition, nor its connection with the glass phase are fully understood. An important characteristic of the relaxation process is the large time domain it spans (about 14 orders of magnitude), which is the reason why more than one technique is usually required to cover the whole domain. In recent years neutron scattering [1] as well as polarized and depolarized light scattering [2] experiments have been able to explore the small viscosity region of some supercooled liquids (i.e., $10^{-2}-10^{2}$ poise) and have shown that the stretched behavior of the relaxation function previously seen at lower frequencies (or longer times) at lower temperature persists in that viscosity range. A superposition of uncorrelated relaxation times could be at the origin of such spectra [3], but nonlinear relaxation processes as described by mode coupling theory [4] (MCT) also lead to stretching in the relaxation function. MCT is also able to describe the dynamics of the supercooled phase of fragile glass-forming liquids for relatively short relaxation times and low viscosities (typically $\tau<10^{-8}$ s or $\eta<100$ P). Until now the origin of this stretching has been a matter of intense discussion [5].

Characterization of this relaxation process, called the structural relaxation process, requires a knowledge of at least 3 to 4 orders of magnitude in the time or frequency domain. However, in a Brillouin scattering experiment, the accessible frequency domain is less than two decades, so that it is generally not possible to study the full relaxation dynamics. Nevertheless, the viscoelastic behavior of supercooled liquids produces a characteristic signature in the Brillouin spectra [6]: when the temperature decreases and the characteristic time of the structural relaxation increases from values typical of a liquid (10^{-12} s) up to values typical of a solid (10^{3} s), the Brillouin lines shift continuously to higher frequencies and their widths go through a maximum, while the central component narrows continuously.

Although Brillouin spectra only provide indirect access to the characteristics of the structural relaxation process, a viscoelastic description introducing structural relaxation through frequency-dependent transport coefficients [6], can determine the characteristic parameters of the relaxation function from the fit to the experimental data. Unfortunately, it was shown in several organic liquids that Brillouin spectra can be well-described using different relaxation functions, in particular functions involving different stretching parameters [7]. This lack of uniqueness can be overcome by introducing stretching parameters extracted from independent experiments, thus assuming implicitly that the relaxation functions of all the relevant variables behave in the same way. So far, this assumption has not been proved theoretically. Nevertheless, it is known empirically that relaxation functions obtained through different experimental techniques can give similar stretching parameters [8]. One question we shall address here is whether, in spite of the intrinsic limitations of the Brillouin scattering technique, it is possible to find a more precise signature of the relaxation function itself by combining different scattering geometries.

$ZnCl_2$ is one of the simplest glass-forming molten salts. Because of this simplicity and of quite low glass and melting temperature ($T_g=102$ °C, $T_m=323$ °C), it has been extensively studied. In addition to classical thermodynamic and viscosity measurements [9,10], the structures of the vitreous and liquid phases were studied by x-ray [11] and neutron [12] diffraction and by Raman spectroscopy [13]. Dynamic properties have been studied by ultrasonic [10] and light scattering [14–20] techniques. More recently an extensive study of liquid $ZnCl_2$, combining molecular dynamics techniques and instantaneous normal mode analysis, was able to

*Present address: PMC, Université Pierre et Marie Curie, 4 Place Jussieu, 75252 Paris Cedex 05, France.

yield insight into the nature of the vibrational modes seen in the spectra of this liquid above the relaxational frequency domain [21].

The structure of glassy and liquid $ZnCl_2$ consists of closely packed Cl^- anions where the small Zn^{2+} cations occupy tetrahedrally coordinated sites. The Cl^- ions shield the Zn^{2+} ions very effectively while linking the tetrahedra through a mainly cornersharing structure. This restricts the mobility of both ions, as can be seen in transport coefficients such as the viscosity which is unusually high [9,10].

An early ultrasonic absorption study [10] yielded values for the elastic moduli, the viscosity, and the relaxation times. Different longitudinal Brillouin scattering studies [14–18] indicate a strong coupling between the longitudinal acoustic mode and the structural relaxation. In four of them [14–17], the analysis of the spectra was performed assuming a pure Debye relaxation process, thus allowing extraction of the infinite longitudinal sound velocity, elastic modulus, and relaxation time. One of these studies [16] explored a wide range of angles, so that the parameters obtained were global ones, optimized simultaneously over all the angles. A large frequency range depolarized light scattering (DLS) study [19] performed by some of us showed a distinctly non-Lorentzian relaxation peak in the susceptibility spectrum, together with a pronounced Boson peak around 20 cm^{-1}. However, no higher frequency relaxation contributions, in the sense of either the Johari-Goldstein β relaxation [22(a)] or the so-called β fast relaxation [22(b)], could be detected in the susceptibility spectra, in contrast to what is often observed in fragile glass-forming liquids. A photon correlation spectroscopy (PCS) study of $ZnCl_2$ [20] was carried out between 120 and 180 °C, showing that the structural α relaxation exhibits a nonexponential behavior in the time domain. Comparing these two experiments, one finds that the stretching parameter slightly increases with temperature, varying from $\beta_K = 0.66$ to $\beta_K = 0.81$ between 120 and 650 °C (β_K is the exponent of the stretched exponential, or Kohlrausch, function, the associated relaxation time being τ_K).

In this paper we report a series of light scattering experiments performed with different geometries and polarizations: backscattering and small angle VV experiments, and 90° VH experiments. The two VV experiments probe longitudinal phonons with wave vectors differing by one order of magnitude. The VH experiments probe the transverse waves, which can propagate in a normal or supercooled liquid provided that the frequency of the probe and the viscosity of the medium are high enough. With the help of results previously obtained in VH backscattering geometry [19], we shall demonstrate that a consistent description of these four experiments can be given assuming that all the relevant relaxation processes are described by stretched exponentials characterized by the same stretching coefficient.

The paper is organized as follows: in Sec. II the relevant theoretical background is briefly summarized. The experimental results and the fitting methods are described in Sec. III. We compare our data to previous ultrasonic and Brillouin data, as well as to static viscosity measurements, and discuss the consistency of our results in Sec. IV. The paper ends with a brief conclusion (Sec. V).

II. HYDRODYNAMIC THEORY AND PREVIOUS RESULTS

A. Density fluctuations and longitudinal phonon dynamics

The main contribution to the polarized intensity in the Rayleigh–Brillouin region of a simple fluid of isotropic particles arises from the density fluctuations at very small wave vectors ($q \sim 10^{-3}$ Å^{-1}). From the classical linearized equations of hydrodynamics [6], the spectral distribution of scattered light is derived to be $I(\omega) = I_0 S(q,\omega)$, where

$$S(q,\omega) = \frac{1}{\pi}\frac{1}{\omega}\mathrm{Im}\{\omega^2 - \omega_0^2 - i\omega q^2 D_v\}^{-1}, \tag{1}$$

where the density fluctuations appear as a Brillouin doublet caused by adiabatic pressure fluctuations. In Eq. (1), $\omega_0 = C_0 q$ is the limiting low-frequency adiabatic relaxed sound frequency, C_0 being the adiabatic relaxed sound velocity, q is the scattering wave vector, and D_v is the frequency-independent longitudinal viscosity. Here heat diffusion effects can and will be neglected.

The D_v coefficient in Eq. (1) usually represents the contribution of anharmonic processes which ensure the return to equilibrium of the fluid after an external density (or temperature) perturbation. In simple liquids, the characteristic relaxation time of this dynamics is of the order of 10^{-12} s, and $q^2 D_v$ is equivalent to a frequency independent damping of the Brillouin lines which have typical frequencies of 10 GHz. In viscoelastic liquids, this characteristic time increases so much with decreasing temperature that in some temperature domain, the structural relaxation time becomes of the same order of magnitude as the inverse of the Brillouin frequency. In this case, the coupling of the structural relaxation dynamics with the acoustic waves yields the specific signature of the relaxation process mentioned in the Introduction. As first recognized by Mountain [23], this behavior can be described within the hydrodynamic theory by introducing a frequency-dependent generalized viscosity:

$$\eta(\omega) = \int dt\ \eta(t)\exp(-i\omega t). \tag{2}$$

The relaxing viscosity described by Eq. (2) can be interpreted as a frequency-dependent loss mechanism. $S(q,\omega)$ is given by

$$S(q,\omega) = \frac{1}{\pi}\frac{1}{\omega}\mathrm{Im}\{\omega^2 - \omega_0^2 - i\omega q^2\gamma_0 - i\omega q^2 D_v(\omega)\}^{-1}, \tag{3}$$

where $D_v(\omega)$ is the frequency-dependent longitudinal kinematic viscosity, related to $\eta(\omega)$ by $D_v(\omega) = \eta(\omega)/\rho$ and $\gamma_0 q^2$ represents the fast processes responsible for the ''normal'' linewidth, which persist in the glass phase.

B. Detection of the transverse modes

When the relaxation time of the shear viscosity is long enough, transverse modes can propagate in a fluid at high enough frequency, producing transverse components in the

depolarized (VH) Brillouin spectrum. Direct optical coupling to these TA modes via the Pockel's coefficient is possible, but is expected to be very weak. In molecular liquids formed of anisotropic molecules, the dominant VH scattering mechanism has been identified long ago [24]: transverse modes couple to small angle molecular rotations, which are themselves at the origin of the fluctuations of the anisotropic part of the local dielectric tensor of the fluid. The $ZnCl_2$ case is more complex since liquid $ZnCl_2$ has a network structure in which no molecular unit can be isolated. Nevertheless, the structural tetrahedral units are found to be rather long-lived [12,21], and their highly polarizable Cl^- corner ions can couple light to orientational motions of the tetrahedra. In such a case, one can attempt to apply to this liquid a recently formulated analysis [25] of the depolarized light scattering spectra of the transverse waves in supercooled liquids, which generalizes Wang's viscoelastic theory [26] and Quentrec's two variables theory [27] of light scattering by transverse modes in molecular liquids.

This generalization takes into account the coupling between the center of mass and orientational motions, and retardation effects on all the friction terms. This leads after simplification to the following expressions for the isotropic and anisotropic spectral intensities $I_{\rm iso}(\omega)$ and $I_{\rm ani}(\omega)$:

$$I_{\rm iso} \propto 1/\omega \, {\rm Im}\left[\frac{1}{\omega^2-\omega_0^2-i\omega q^2\gamma_0-i\omega\rho_m^{-1}q^2 D_{\rm LT}(\omega)}\right], \tag{4a}$$

$$I_{\rm ani} \propto 1/\omega \, {\rm Im}\left[R(\omega)+\cos^2\,\theta/2\,\frac{\Lambda q^2\rho_m^{-1}R(\omega)^2}{\omega^2-i\omega\rho_m^{-1}q^2\eta_{\rm ST}(\omega)}\right], \tag{4b}$$

where ρ_m is the mass density, θ is the scattering angle, $D_{\rm LT}(\omega)$ and $\eta_{\rm ST}(\omega)$ are, respectively, the total longitudinal and shear viscosities, and Λ being a factor representing the magnitude of the coupling between the shear and an orientational variable. The term $R(\omega)$ which appears twice in Eq. (4b) describes the dynamic of the orientational variable which is directly detected in the anisotropic spectrum (first term) and which is the detection mechanism of the transverse phonons (second term).

In these equations, the total longitudinal and shear viscosities, $D_{\rm LT}(\omega)$ and $\eta_{\rm ST}(\omega)$, are related to the usual longitudinal, shear and bulk viscosities and to the orientational relaxation function $R(\omega)/\omega$ by

$$\omega D_{\rm LT}(\omega)=\omega D_l(\omega)-(4/3)\Lambda R^2(\omega)/[1-R(\omega)], \tag{5a}$$

$$\omega D_l(\omega)=\omega\eta_b(\omega)+(4/3)[\omega\eta_s(\omega)], \tag{5b}$$

$$\omega\eta_{\rm ST}(\omega)=\omega\eta_s(\omega)-\Lambda R^2(\omega)/[1-R(\omega)], \tag{5c}$$

where $D_l(\omega)$, $\eta_b(\omega)$, and $\eta_s(\omega)$ are, respectively, the frequency-dependent longitudinal, bulk, and shear viscosities without translation-rotation coupling (i.e., bare viscosities related only to motion of the centers of mass).

C. Frequency dependence of the transport coefficients

The three preceding viscosities are special cases of transport coefficients, $\sigma(\omega)$, which are Laplace transforms of correlation functions. Assuming for these functions a Debye relaxation mechanism:

$$\sigma(\omega)=\sigma(0)/(1+i\omega\tau_s) \tag{6}$$

which is the Maxwell formulation of viscoelasticity [28].

Several approaches are possible to obtain more realistic representations of these correlation functions, in particular of their long time behavior. Although solving nonlinear coupled equations of motion related to microscopic densities self-consistently is the elegant method used in the mode coupling theory [4], this approach was not found [19] relevant in the analysis of the DLS susceptibility spectra of molten $ZnCl_2$. Also the use of $R(\omega)$ to deduce the expression of $D_{\rm LT}(\omega)$ [7] turned out to be impossible, as was already the case in other systems [29]. The simplest method (which is most often followed) is to introduce empirical correlation functions with their associated frequency-dependent transport coefficients. Correlation functions are usually approximated by a stretched exponential and the corresponding Laplace transform of this function can be conveniently approximated by the Cole-Davidson function:

$$m(\omega)=\frac{-im(0)}{\omega\beta_{\rm CD}\tau_{\rm CD}}\left[1-\left(\frac{1}{1+i\omega\tau_{\rm CD}}\right)^{\beta_{\rm CD}}\right], \tag{7a}$$

$m(\omega)$ generalizing Eq. (6) and being, for $\beta_{\rm CD}=1$, the Lorentzian function, the corresponding parameters $\beta_{\rm CD}$ and $\tau_{\rm CD}$ being related to β_K and τ_K [30].

A previous study [19] of the depolarized backscattering of $ZnCl_2$, analyzed with [Eq. (4b)] showed that a Cole-Davidson form could be chosen for the uncoupled rotational dynamics term, $R(\omega)$:

$$R(\omega)=R_0\left\{1-\left(\frac{1}{(1+i\omega\tau_r)}\right)^{\beta_{\rm CD}}\right\}. \tag{7b}$$

Equation (7b) thus allows for an experimental determination of the corresponding $\beta_{\rm CD}$ and $\tau_r(T)$. In the present paper we shall compare the results obtained by fitting the different Brillouin spectra with two different expressions for $D_{\rm LT}(\omega)$ and $\eta_s(\omega)$:

(i) either Lorentzian functions:

$$D_{\rm LT}(\omega)=\Delta^2\frac{\tau_l}{(1+i\omega\tau_l)}, \tag{8a}$$

$$\eta_s(\omega)=G_\infty\frac{\tau_s}{(1+i\omega\tau_s)} \tag{8b}$$

where G_∞ is the infinite frequency shear modulus,

(ii) or Cole-Davidson functions:

$$D_{\rm LT}(\omega)=\frac{(-i)\Delta^2}{\omega}\left\{1-\left(\frac{1}{(1+i\omega\tau_l)}\right)^{\beta_{\rm CD}}\right\}, \tag{9a}$$

$$\eta_s(\omega)=\frac{(-i)G_\infty}{\omega}\left\{1-\left(\frac{1}{(1+i\omega\tau_s)}\right)^{\beta_{\rm CD}}\right\}. \tag{9b}$$

Referring to Eqs. (5a) and (5b), we see that the longitudinal damping function $D_{\mathrm{LT}}(\omega)$ includes contributions from the shear-orientation coupling [second term of the right-hand side in Eq. (5a)] in addition to the usual contributions from bulk and shear viscosities. In the present analysis, however, we shall not attempt to separate these contributions but shall utilize the simpler conventional formulation for $D_{\mathrm{LT}}(\omega)$ of Eq. (9a).

From the low frequency limit of Eq. (9b), one sees that the static shear viscosity coefficient, η_s, is equal to

$$\eta_s = \beta G_\infty \tau_s , \tag{10a}$$

which reduces, in the Lorentzian case ($\beta = 1$) to the usual Maxwell relation:

$$\eta_s = G_\infty \tau_s . \tag{10b}$$

The high frequency limit of Eqs. (4b), (5c), (7), and (9b) gives rise to a transverse phonon propagating with a velocity $v_t = r[G_\infty/\rho_m]^{1/2}$ where r is a reduction factor which originates from the rotation translation coupling term. The latter coefficient decreases the value of the high frequency transverse wave velocity predicted by the Maxwell theory of viscoelasticity and is given by

$$r = [1 - \Lambda R_0^2 G_\infty^{-1}(1 - R_0)^{-1}]^{1/2}. \tag{11}$$

D. Formalism in previous studies

All the previous results [14–17] concerning the longitudinal sound velocities and elastic moduli of molten $ZnCl_2$ were obtained assuming a Debye single relaxation time process. In one case, where several scattering geometries were studied [16], the consistency of the analyses required the additional introduction of a second contribution to $D(\omega)$:

$$D'_{\mathrm{LT}}(\omega) = \Delta^2 \frac{\tau_l}{1 + \omega^2 \tau_l^2} + D_v , \tag{12a}$$

$$D''_{\mathrm{LT}}(\omega) = -\Delta^2 \frac{\omega \tau_l^2}{1 + \omega^2 \tau_l^2} - D_v \omega \tau_f . \tag{12b}$$

The D_v term being an approximation for a fast relaxation process not included in the first Lorentzian term.

III. EXPERIMENTAL PROCEDURES AND RESULTS

A. Experiment

Samples of $ZnCl_2$ were prepared according to a method described in Ref. [16] and used in Ref. [19]. When melted and then slowly cooled, the samples crystallize around 280 °C, providing a limited supercooled range of about 40 °C. The samples were kept in cylindrical cells sealed under vacuum (square cells always break at the melting point of $ZnCl_2$). Experiments were performed with a Sandercock-type tandem Fabry-Perot described elsewhere [31]. The light source was a Coherent Innova 90 A^+ laser operating in single mode at 514.5 nm. Several geometries and polarizations were used and, for each of them, one or two different free spectral ranges (f.s.r.) were used: 18.5 and 7.5 GHz for the VV near backscattering geometry [$\theta = 171°$]; 5 GHz for the VV near forward scattering [$\theta \sim 12°$] and 10 GHz for the VH 90° experiment. VV spectra were collected between 300 and 650 °C in backscattering and between 300 and 550 °C for the small angle geometry. VH spectra were recorded between 320 and 400 °C.

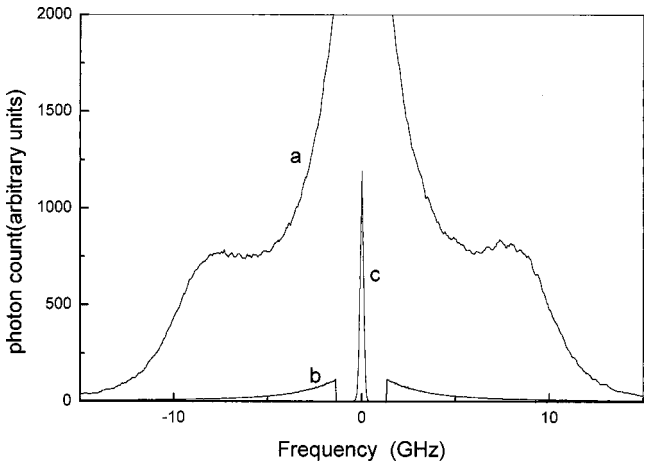

FIG. 1. (a) VV and (b) VH spectra at 500 °C in the same experimental conditions. (c) Instrumental Rayleigh line.

In the backscattering geometry, the polarized light scattering intensity includes contributions coming from both the isotropic and anisotropic parts of the dielectric tensor fluctuations, whereas the VH contribution measured in the same geometry comes only from the anisotropic part:

$$I_{\mathrm{VV}} = I_{\mathrm{iso}} + 4/3 I_{\mathrm{ani}} , \tag{13a}$$

$$I_{\mathrm{VH}} = I_{\mathrm{ani}} \tag{13b}$$

Figure 1, which compares VV and VH near-backscattering spectra taken at 500 °C in the same experimental conditions, shows that, in the region of the Brillouin triplet, I_{VV} is much larger than I_{ani}. The anisotropic contribution to I_{VV} can thus be reasonably neglected, which has been done at all temperatures.

Figure 2 shows VV backscattering spectra for temperatures from 300 to 650 °C. This figure shows the strong coupling which exists between density fluctuations and the α-relaxation process. This coupling is maximum when $2\pi\nu_B\tau_l \sim 1$, around 550 °C in this scattering geometry ($q = 0.0244\,\mathrm{nm}^{-1}$ at $T = 550$ °C), and results in the merging of the Brillouin doublet with the central peak. At this temperature, the Brillouin lines are not resolved.

For the two other experiments, it is necessary to take also into account some specific problems related to scattering at angles different from the backscattering geometry. For analyzing the experiments, the wave vector **q** has to be properly defined. As $q = 2(2\pi n/\lambda)\sin\frac{\theta}{2}$ and $\Delta q = (2\pi n/\lambda)\cos\frac{\theta}{2}\Delta\theta$, where λ is the wavelength of the laser light and n the refraction index, one must have a good knowledge of θ and use as small a $\Delta\theta$ as possible. In these two last experiments, the small $\Delta\theta$ condition was taken into account by using a small

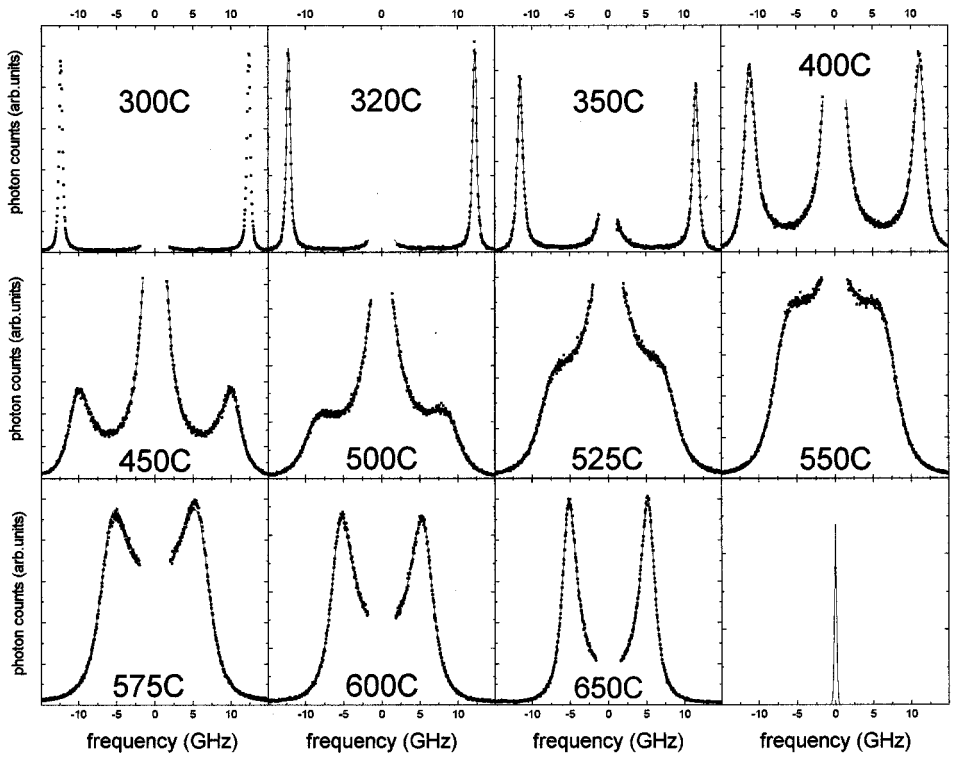

FIG. 2. Thermal evolution of the backscattering VV $ZnCl_2$ spectra: experiment (■), fit with $\beta_{CD}=0.68$ (----). The last panel shows the instrumental function.

aperture compared to the scattering angle itself: we chose $\Delta\theta=10^{-2}$ rad, a value much smaller than in the backscattering case.

In the 12 °VV experiment (Fig. 3), the same thermal behavior as in Fig. 2 is observed; but as the wave vector is about one order of magnitude smaller than in the backscattering case ($q=0.0025\,\mathrm{nm}^{-1}$ at $T=550$ °C), the maximum of the coupling is shifted to lower temperatures, i.e., around 400 °C. At 500 °C, a spectrum typical of a liquid is already obtained, precluding a precise measurement of the relaxation time.

The 90° depolarized VH spectra are shown in Fig. 4 in the temperature range 320–400 °C. At low temperatures, the well-resolved transverse Brillouin lines are the signature of propagative transverse acoustic modes, seen well above the melting point, a feature already observed in $ZnCl_2$ [14] as well as in other inorganic nonfragile glass-forming liquids [32]. When the temperature increases, the transverse Brillouin lines shift to lower frequencies and the damping increases. At 400 °C, the transverse modes appear only as shoulders on both sides of the central line, and at still higher temperatures they totally collapse into it.

B. Fit procedure

VV spectra were analyzed using a conventional nonlinear least-squares fitting procedure to a theoretical function $I(\omega)$ convoluted with a Gaussian function adjusted to fit the apparatus profile. $I(\omega)$ was taken to be

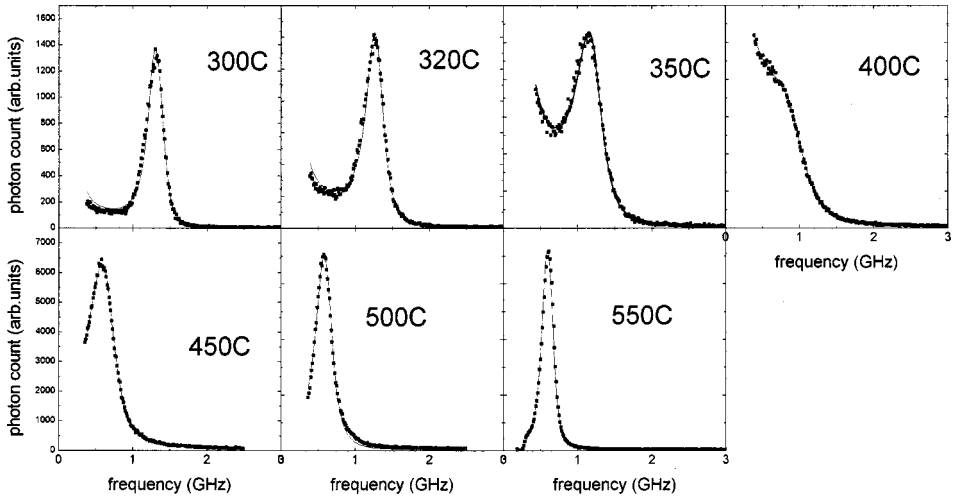

FIG. 3. Thermal evolution of the small angle VV $ZnCl_2$ spectra: experiment (■), fit with $\beta_{CD}=0.68$ (----).

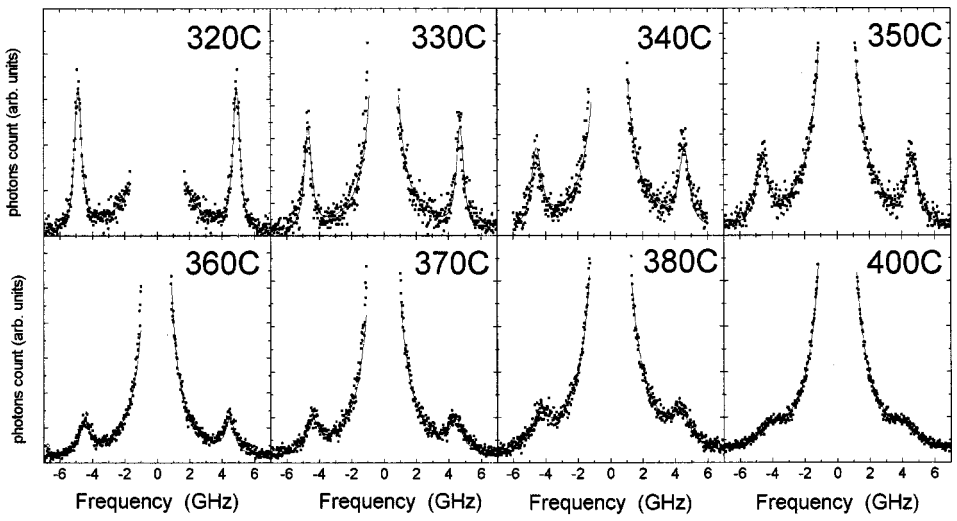

FIG. 4. Thermal evolution of the 90° VH $ZnCl_2$ spectra: experiment (■), fit with $\beta_{CD}=0.68$ (----).

$$I(\omega)=\frac{1}{\pi}\frac{I_0}{\omega}\mathrm{Im}\{\omega^2-\omega_0^2-i\omega q^2\gamma_0-q^2\Delta^2 \times[1-(1+i\omega\tau_l)^{-\beta_{CD}}]\}^{-1}+I_{bg}, \quad (14)$$

where I_0 and I_{bg} are, respectively, the strength of the isotropic contribution to the VV spectrum and the background intensity while Δ represents the strength of the coupling between the α structural relaxation and the longitudinal acoustic phonon. This parameter is related to C_0, the adiabatic relaxed sound velocity and C_∞, the sound velocity at infinite frequency by

$$C_\infty=\sqrt{C_0^2+\Delta^2}. \quad (15)$$

In our fitting procedure, I_0, I_{bg}, C_0, Δ, and τ_l were treated as adjustable parameters and we fixed the values of β and γ_0 as follows. As the fitting procedure does not allow for a determination of β, we used either Eq. (8) ($\beta=1$) as was done for $ZnCl_2$ in previous studies or the mean value of β_{CD} ($\beta_{CD}=0.68$) deduced from our fits to the α peak in the depolarized backscattering spectra [19]. Indeed, one purpose of this analysis is to check whether significant differences in the results can be observed between the use of one or the other value.

TABLE I. Results of the Cole-Davidson fits for the backscattering VV experiment.

	$\beta_{CD}=0.68$				$\beta=1$			
T °C	$\Delta_1=\Delta q$ GHz	τ_l ns	ω_0 GHz	χ^2	$\Delta_1=\Delta q$ GHz	τ_l ns	ω_0 GHz	χ^2
300	10.77	2.19	6.19	1.8	10.77	0.47	6.49	2.4
320	10.68	1.23	6.21	1.4	10.55	0.33	6.24	2.2
350	10.41	0.44	6.12	2.7	9.85	0.16	6.12	3.1
400	10.29	0.13	5.76	2.3	9.83	0.084	5.60	3.1
450	9.80	0.052	5.65	1.4	9.01	0.037	5.69	1.8
500	9.20	0.028	5.38	1.3	8.29	0.023	5.32	1.8
525	8.85	0.022	5.24	1.9	7.94	0.018	5.21	2.3
550	8.43	0.019	5.25	1.4	7.51	0.016	5.21	1.6
575	8.13	0.015	5.21	3.1	7.24	0.013	5.19	3.3
600	7.85	0.012	5.20	2.3	6.97	0.011	5.18	2.3
650	7.34	0.009	5.12	4.9	6.54	0.008	5.11	4.9

The parameter γ_0 was determined by assuming that, in the temperature range of interest, its variation could be neglected. γ_0 was thus deduced from a measurement of the Brillouin linewidths in the glass and in the low temperature supercooled liquid ($T<160$°C) in the same backscattering geometry. The very narrow Brillouin lines were deconvoluted from the instrumental profile yielding $\gamma_0 q^2/2\pi \approx 0.025$ GHz.

We note that C_0 was taken as a free fit parameter although C_0 is known from ultrasonic measurements [10]. Actually, using these values as input parameters, acceptable fits to our data could not be obtained. Gruber and Litovitz [10] pointed out that a small amount of water (3%) still remained inside their sample, which could lead to a slight variation in C_0. Therefore we let C_0 be a free parameter, under the condition that the final values should be compatible with Ref. [10] within the limit of accuracy of that experiment.

Fits to the small angle spectra were done using the same techniques and the same Eq. (14) but the influence of the finite solid angle was taken into account in the fit, by integrating over the q range intercepted by the finite aperture (10^{-2} rad). Moreover, as the cylindrical cell could introduce small variations in the direction of the optical path inside the cell, we also took q as a free parameter. This was done by making use of the values $C_0(T)$ and $\Delta(T)=\sqrt{C_\infty^2-C_0^2}$, obtained from the backscattering VV experiments: at each temperature, the only adjustable parameters left are thus q, the relaxation time τ_{VV}, I_0, and I_{bg}. Actually, the value of q was found to differ by at most, 5%, of the value given by the direct measurement of the angle.

The analysis of the transverse mode spectra is more intricate. Following Eq. (4b), and introducing, as in Eq. (14) an additional temperature-independent scattering mechanism, this profile is given by

TABLE II. Results of the Cole-Davidson fits for the small angle VV experiment.

		$\beta_{CD}=0.68$				$\beta_{CD}=1$			
T °C	Angle degrees	$\Delta_1=\Delta q$ GHz	τ_l ns	ω_0 GHz	χ^2	$\Delta_1=\Delta q$ GHz	τ_l ns	ω_0 GHz	χ^2
300	12					1.14	0.765	0.675	
320	12.3	1.17	1.03	0.655	2.7				
350	12.3	1.34	0.48	0.641	1.3	1.055	0.33	0.64	2.7
400	12.15	1.06	0.17	0.615	2.	0.956	0.14	0.615	2.3
450	12.15	1.03	0.077	0.595	4.5	0.93	0.064	0.595	4.3
500	12.3	1.03	0.044	0.585		0.925	0.037	0.585	
550	13	0.96	0.026	0.59		0.955	0.0175	0.59	

$$I_{\mathrm{ani}}(\omega)\propto\frac{I_0}{\omega}\mathrm{Im}\left[R(\omega)+\cos^2\theta/2\times\frac{\Lambda q^2\rho_m^{-1}R(\omega)^2}{\omega^2-i\omega q^2\eta_{\mathrm{ST}}(\omega)-i\omega\gamma_0 q^2}\right]+I_{\mathrm{bg}}. \quad (16)$$

As in Eq. (4), I_0 and I_{bg} are, respectively, the strength of the anisotropic contribution to the VH spectrum and the background intensity. γ_0, which describes again the contribution of processes intrinsic to the transverse Brillouin lines, was assumed to have the same value as its longitudinal counterpart. The fitting parameters are thus τ_s, Λ, and R_0, in addition to I_0 and I_{bg}. At each temperature $R(\omega)$ was obtained from Eq. (7b), the coefficients β_{CD} and $\tau_r(T)$ being deduced from Ref. [19]. As backscattering VH spectra did not allow one to properly determine $\tau_r(T)$ below 400 °C, values at lower temperatures were inferred from an interpolation between these results and the PCS measurements [20], using a Vogel–Fulcher approximation. For $\eta_s(\omega)$, the two expressions (8b) and (9b) were used with, in the second case, the β_{CD} value obtained from Ref. [19].

C. Results

1. Longitudinal modes

The parameters of the fit obtained for $\beta=1$ and $\beta_{\mathrm{CD}}=0.68$ are collected in Tables I–III together with the corresponding confidence factor χ^2 for the VV backscattering, VV small angle, and VH 90° geometries. Fits are shown in Figs. 2–4. Let us stress that both values of β yield apparently equally good fits. The difference is mostly a numerical one: for VV backscattering (Table I) below 575 °C, the χ^2 values are always lower for the fit made with $\beta_{\mathrm{CD}}=0.68$ than for the fit made with $\beta=1$ and this difference increases with decreasing temperatures. This temperature effect could be expected: indeed, the values reported in Table I show that the product $2\pi\nu_B\tau_l$, where ν_B is the frequency of the Brillouin peak, is of the order of unity around 500 °C. As the difference in the shape of the relaxation functions for the two different values of β is only important for $2\pi\nu_B\tau_l\gg1$, it is mostly at low temperature that the two relaxation functions will produce different spectral shapes of the Brillouin lines. The relaxed and nonrelaxed sound frequencies ω_0 and $\omega_\infty=[\omega_0^2+\Delta^2q^2]^{1/2}$ deduced from the backscattering experiments, as well as the corresponding elastic moduli $M_0=\omega_0^2q^{-2}\rho_m$ and $M_\infty=\omega_\infty^2q^{-2}\rho_m$ are shown in Fig. 5. The sound velocities, C_0 and C_∞, have a smooth temperature variation which can be fitted by the linear interpolation formulas:

$$C_0=[1150-0.53T(^\circ\mathrm{C})]\,\mathrm{m\,s^{-1}} \quad (17a)$$

for both β values, while $C_\infty(T)$ depends on β:

TABLE III. Results of the Cole-Davidson fits for the 90° VH experiment.

			$\beta_{CD}=0.68$					$\beta=1$				
T °C	τ_r ns	ρ K gm^{-3}	τ_{sCD} ns	Λ Pa	χ^2	Eta_0 Pa*E9	η_s poise	τ_s ns	Λ Pa	χ^2	Eta_0 Pa*E9	η_s poise
320	4.1	2517	1.02	5.34	1.1	3.84	26.6	0.41	2.12	1.1	3.35	13.6
330	3.1	2513	0.89	4.41	1.8	3.46	21.0	0.39	2.17	1.8	3.08	11.5
340	2.7	2508	0.54	3.92	2.1	3.28	12.1	0.27	1.57	2.1	2.88	7.8
350	2.5	2504	0.50	2.49	2.6	3.33	11.3	0.23	1.18	2.5	2.99	6.8
352	2.5	2503	0.48	2.85	1.4	3.10	10.1	0.22	1.20	1.4	2.87	6.0
360	1.5	2499	0.46	2.35	2.1	3.11	9.8	0.22	1.65	2.1	3.14	6.1
370	1.3	2495	0.38	1.83	1.7	3.04	7.9	0.18	1.51	1.7	2.71	4.7
380	1.1	2490	0.29	2.74	1.7	2.99	6.0	0.13	1.57	1.7	3.22	3.9
390	0.95	2486	0.28	0.94	1.1	2.44	4.7	0.13	0.75	1.1	2.71	3.2
400	0.87	2481	0.20	0.84	1.8	2.83	3.8	0.08	2.24	1.8	3.64	2.3

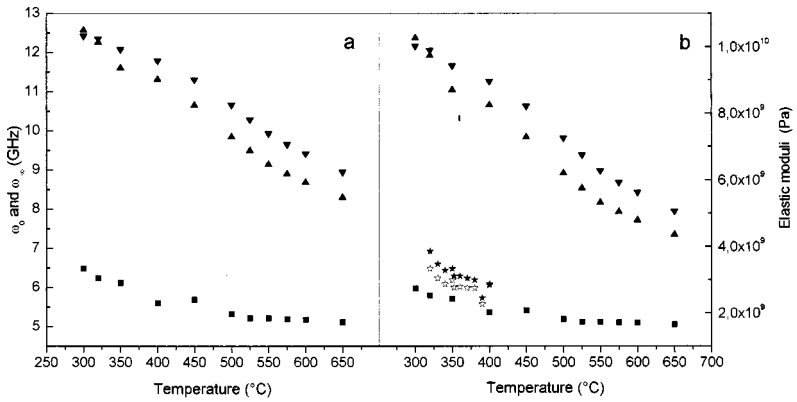

FIG. 5. Results derived from the present experiment. (a) Relaxed longitudinal sound frequency ω_0: (■); nonrelaxed longitudinal sound frequency ω_∞: $\beta=1$ (▲); $\beta_{CD}=0.68$ (▼); (b) relaxed longitudinal elastic modulus (■); nonrelaxed longitudinal elastic modulus: $\beta=1$ (▲), $\beta_{CD}=0.68$ (▼); shear modulus: $\beta=1$ (☆), $\beta_{CD}=0.68$ (★).

$$\beta=1, \quad C_\infty=[2574-1.93T(^\circ\mathrm{C})]\,\mathrm{m\,s^{-1}}, \tag{17b}$$

$$\beta_{CD}=0.68, \quad C_\infty=[2538-1.66T(^\circ\mathrm{C})]\,\mathrm{m\,s^{-1}}. \tag{17c}$$

The corresponding relaxation times, $\tau_l(T)$ are shown in Fig. 6 and depend slightly on the value of β. Their thermal variations can be represented by an Arrhenius law:

$$\beta=1, \quad \tau_l=8.51\times10^{-6}\exp(6187/T)(\mathrm{ns}), \tag{18a}$$

$$\beta_{CD}=0.68, \quad \tau_l=4.27\times10^{-7}\exp(8395/T)(\mathrm{ns}). \tag{18b}$$

In the small temperature range available here, the most important role of the small angle polarized experiment was to check the consistency of the values found for the relaxation times, τ_l, for both values of β. In this experiment the confidence factors are rather poor. For the highest temperatures the error is very large, because the Brillouin lines are very close to the central line. Nevertheless, Figs. (6a) and (6b) show that the agreement between the backscattering and the small angle τ_l values obtained with $\beta_{CD}=0.68$ is better at all temperatures, except 550 °C, than with $\beta=1$. The good agreement between the two sets of values is a validation of the fitting procedure of the polarized Brillouin spectra even for relaxation times one order of magnitude larger than the characteristic time of the probe (inverse of the frequency of the Brillouin peak): the analysis of the Brillouin lines can give a reliable estimate of the relaxation times even far from the region where the condition $2\pi\nu\beta\tau\sim1$ is fulfilled (this corresponds to $\tau_l=0.017$ ns at 550 °C for the backscattering and to $\tau_l=0.17$ ns at 400 °C for the small angle scattering experiments).

2. Transverse modes

Values of the parameters and of the χ^2 factors are collected in Table III. χ^2 values do not appreciably differ for the two β values. Figure 5(b) shows the temperature variation of the elastic shear infinite elastic modulus, G_∞, while the corresponding relaxation times, τ_s, are shown in Fig. 6. The values of G_∞ obtained with both values of β differ only slightly (~5%), showing the stability of this quantity in the fit. This is not surprising as the value of this parameter is basically determined by the frequency of the maximum of the Brillouin line. Linear fits to the experimental points give

$$\beta_{CD}=0.68, \quad G_\infty=6.3\times10^9-8.97\times10^6T(^\circ\mathrm{C})\mathrm{Pa}, \tag{19a}$$

$$\beta=1, \quad G_\infty=6.03\times10^9-8.75\times10^6T(^\circ\mathrm{C})\mathrm{Pa}. \tag{19b}$$

At each temperature, the corresponding shear relaxation times, τ_s, are close to the longitudinal relaxation times, τ_l, obtained with the same value of β, showing that, in this specific case, shear and longitudinal relaxation times are

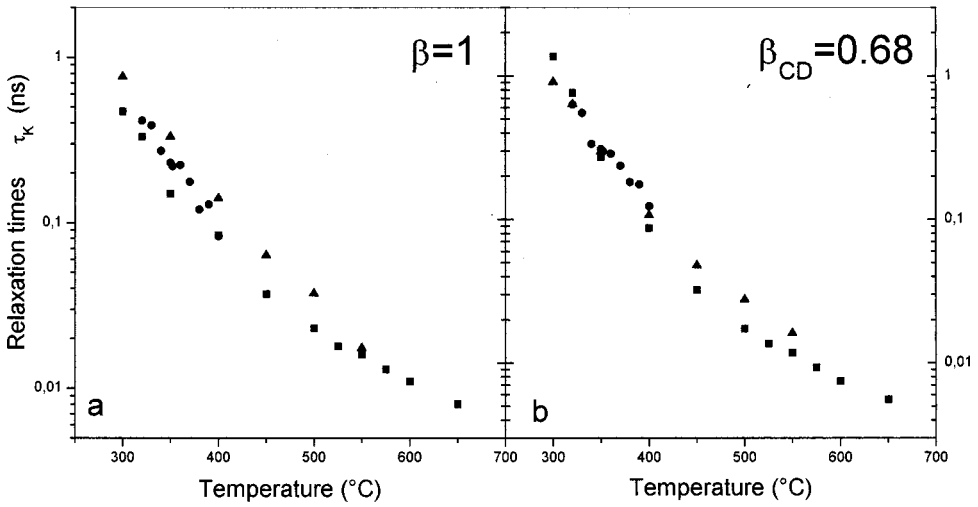

FIG. 6. Results derived from the present experiment: relaxation times for $\beta=1$ (a) and $\beta_{CD}=0.68$ (b): τ_l Backscattering VV (■); τ_l small angles VV (▲); τ_s 90° angles VH (●).

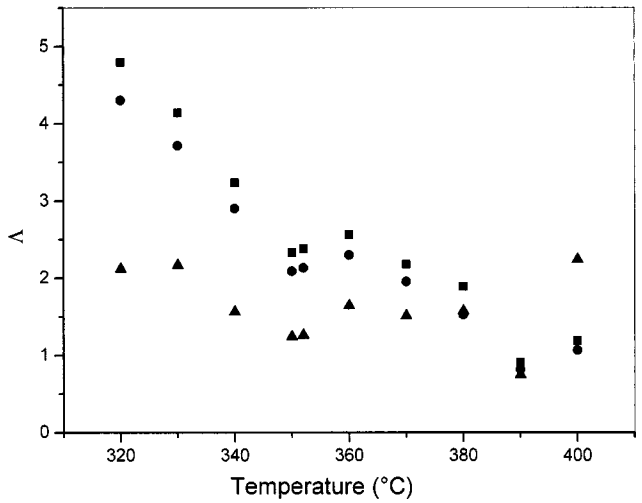

FIG. 7. Thermal variation of Λ in the fit of the transverse modes with fixed $R_0:\beta=1$, $R_0=0.52$ (▲); $\beta_{CD}=0.68$, $R_0=0.55$ (■); $\beta_{CD}=0.68$, $R_0=0.61$ (●).

equal within the error bars. While performing the fit procedure we noticed that some parameters, in particular Λ and R_0 were strongly correlated, an expected feature due to the large number of free parameters. In a first fit with Λ and R_0 free, the variation of the latter was fairly small. Thus we performed a second fit in which we fixed R_0 at its mean value in the first fit. The variation of the other parameter, Λ, is reported in Fig. 7. For $\beta_{CD}=0.68$, $R_0=0.55$, the value of Λ decreases regularly with increasing temperature, while, with $\beta=1$ and $R_0=0.52$, Λ has a rather erratic variation. An increase of Λ with decreasing temperature had to be anticipated: Λ measures the importance of the shear-rotation coupling which is expected to decrease for increasing temperature because of the corresponding decrease of the density. The values of this parameter have large error bars because of the relative weakness of the coupling term in the denominator of Eq. (16): the value of the corresponding r coefficient [Eq. (11)] is, indeed, never lower than 0.95 which means that the second term in the right-hand side reaches only about 5% of the bare shear viscosity term. The similarity between the values of τ_l and τ_s, as well as the small values of $1-r$, are an *a posteriori* justification of the method we have followed to analyze the longitudinal Brillouin spectra where we have ignored the separation of the total frequency-dependent viscosity into different terms, one of them representing the coupling with orientational motions. We have also verified the stability of G_∞ and τ_s in the fit by repeating the fitting procedure with another fixed value for R_0 ($R_0=0.61$): a mean relative variation of 0.03 for G_∞ and 0.04 for τ_s was obtained whereas it reaches 0.12 for Λ.

IV. DISCUSSION

A. Elastic moduli

Figure 8 compares our results for the speeds of sound [Eq. (8a)] and elastic moduli [Eq. (8b)] with previous data obtained from different Brillouin [14–17] and ultrasonics [10] experiments. First of all, whatever the experimental procedure and the fitting method, the relaxed sound velocities, C_0, and their thermal variations are very similar; in particular, our values agree, within a reasonable error bar, with the direct sound velocity measurement [10], with an approximately constant difference throughout the whole temperature domain. This is not the case for the infinite frequency sound velocity; $C_\infty(T)$ is more sensitive to the hypotheses made in the fit. This is also true for its dependence on the value of β. The changes fall outside of the standard error defined as the dispersion of all the experimental data obtained with $\beta=1$. Similar results are obtained for the elastic moduli.

The shear infinite elastic moduli, $G_\infty(T)$, obtained in this work are much larger than values given by Gruber and Litovitz [10] [Fig. 8(b)]. This is in line with measurements of the transverse Brillouin frequency made by Knape [14]. The rea-

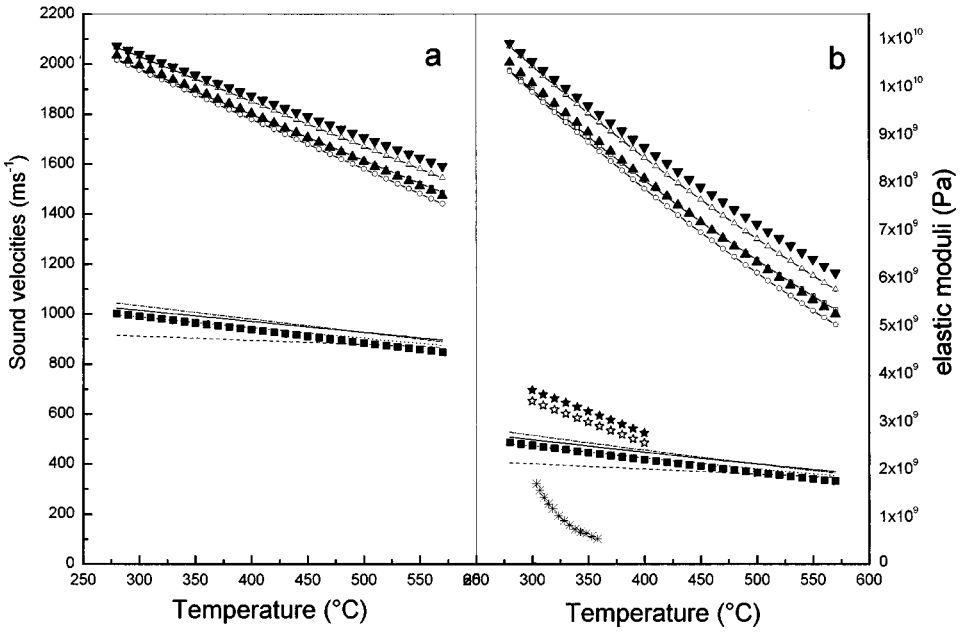

FIG. 8. Comparison of the present results (same symbols as in Fig. 5) with other measurements: (a) Sound velocities C_0: Ref. [10] (—); Ref. [15] (----); Ref. [14] (· · · ·); Ref. [16] (—·—·—·—); C_∞: Ref. [14] (–○–); Ref. [16] (–△–); (b) Longitudinal elastic moduli M_0 and M_∞, same as (a) and shear elastic modulus G_∞, Ref. [10] (*).

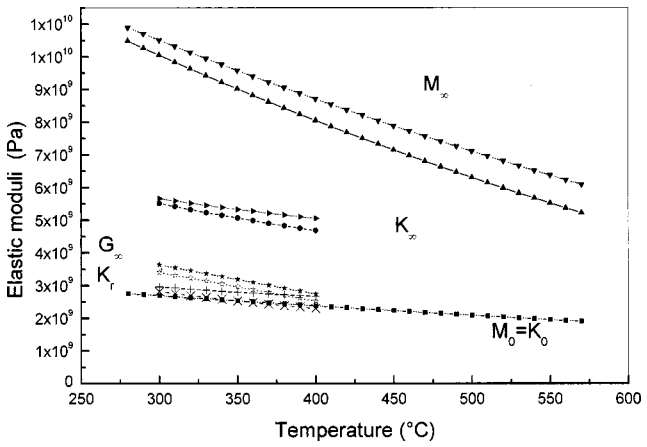

FIG. 9. Elastic moduli derived from the present experiment: M_∞, $\beta=1$ (▲), $\beta_{CD}=0.68$ (▼); K_∞, $\beta=1$(●)$_\infty$, $\beta_{CD}=0.68$ (▶); M_0 (■); G_∞, $\beta=1$ (☆), $\beta_{CD}=0.68$ (★) K_r, $\beta=1$ (×), $\beta_{CD}=0.68$ (+).

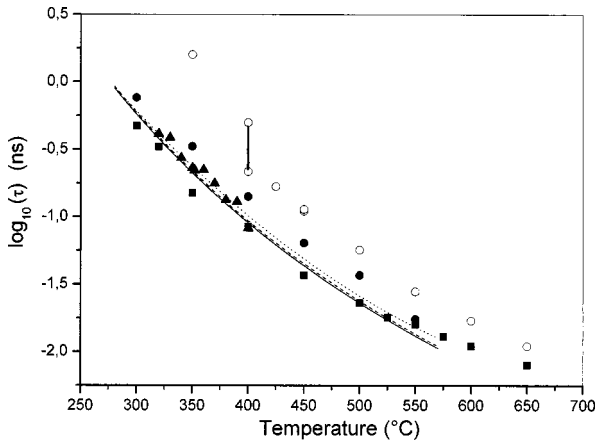

FIG. 10. Relaxation times: comparison with other measurements obtained with the $\beta=1$ assumption: τ_{VV}, backscattering (■); τ_l, small angle scattering (●); τ_s (▲); Ref. [16](—); Ref. [14] (– – –); Ref. [15] (· · · ·). For the sake of comparison, τ_r from Refs. [19] and [20] (○) with $\beta_{CD}=0.68$ are also included: the two values shown for $T=400\,°C$ give an estimate on the error bars on these values at the lowest temperature.

son for such a difference is probably that determining G_∞ using ultrasonic measurements is only possible through an extrapolation scheme; on the contrary, Brillouin measurements of the transverse mode frequency give a direct access to the Brillouin shear modulus, which provides, by itself, a lower limit to the infinite frequency shear modulus.

From the measurements of the different elastic moduli, one can estimate the infinite frequency bulk [33,34] (or compressional) modulus $K_\infty=M_\infty-\frac{4}{3}G_\infty$, [see Eqs. (5b), (9), and (15)] as well as the relaxational modulus $K_r=K_\infty-M_0$ which is the contribution of the structural rearrangement to K_∞. The different moduli are shown in Fig. 9 where one sees that G_∞ and K_r have very similar values. This similarity is suggestive of the following idea. In $ZnCl_2$, the $ZnCl_4^{2-}$ tetrahedra are mostly corner-sharing, and each of them is nearly incompressible: an isotropic compression will mainly tend to bend the Zn—Cl—Zn bonds and the same bending is the only source of the shear modulus, G_∞. This bending should thus give an equal contribution to G_∞ and K_r.

B. Relaxation times

The relaxation times extracted from the different analyses performed with the $\beta=1$ assumption are shown in Fig. 10. The agreement between the times extracted from the different Brillouin experiments is excellent. The small dispersion observed in these data comes undoubtedly from the differences in the experiments and this dispersion mostly represents the experimental errors. As already mentioned, the shear relaxation time τ_s, also shown in Fig. 10, is close to τ_l.

The relaxation times τ_r, extracted from backscattering DLS [19] and PCS [20] experiments are shown in Fig. 10. Although the determination of τ_r by DLS is quite poor at and below 400 °C, as can be seen by the large error bar, τ_r is substantially larger than τ_l and the thermal variations are different. Moreover, both DLS [19] and PCS [20] experiments detect in a direct way a relaxation function characterized by a non-Debye stretching parameter. This favors an analysis of the Brillouin lines with $\beta=0.68$. The results are summarized in Fig. 11 where the two τ_l and the τ_s values have been multiplied by 2.43 in order to demonstrate the following additional feature: the ratio τ_r/τ_l (and τ_r/τ_s) is practically constant ($\sim$2.43) through the whole temperature range where it can be measured, i.e., the thermal variations of τ_l and τ_s determined with $\beta_{CD}=0.68$ are the same as that of τ_r. (Let us notice that a better agreement between these three variations could probably be obtained by letting β take a slightly smaller value, an exercise we did not attempt to do in order to keep the number of adjustable parameters as low as possible.) This type of scaling between different relaxation times is predicted by MCT [4] and is presumably more general.

C. Viscosity

Using Eq. (10a), and the values of G_∞ and τ_s taken from Table III, one can compute the static shear viscosities, η_s,

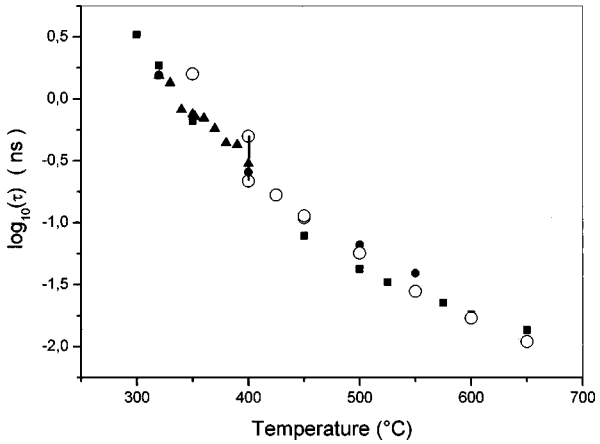

FIG. 11. Comparison between relaxation times obtained with $\beta_{CD}=0.68$:$2.43\tau_l$, backscattering (■); $2.43\tau_l$, small angle scattering (●); $2.43\tau_s$ (▲); τ_r from Refs. [19] and [20] (○).

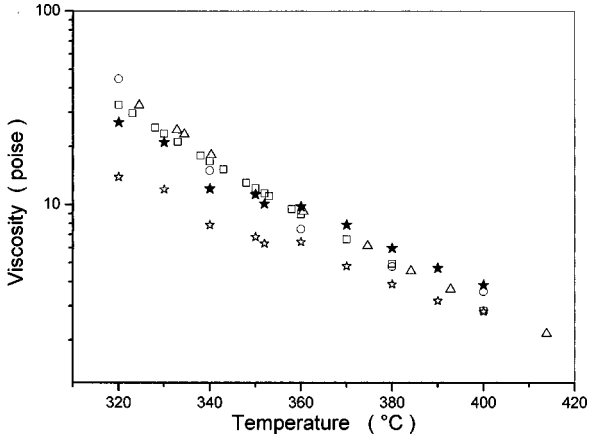

FIG. 12. Comparison between calculated viscosities and direct measurements. $\beta=1$: (☆); $\beta_{CD}=0.68$ (★); Ref. [10] (□); Ref. [9(a)] (○), Ref. [9(b)] (△).

up to 400 °C. The results are shown in Fig. 12, together with the results of three independent series [9,10] of direct measurements performed between 320 and 400 °C. Those three sets of measurements are in excellent agreement in the whole temperature range, with an experimental accuracy estimated [10] to be within 1.5%. They agree very well with the values deduced from Eq. (10a) with $\beta_{CD}=0.68$. On the contrary, a clear discrepancy with the direct measurement, both in absolute value and thermal variation, appears if one uses the values derived from the $\beta=1$ fits.

V. CONCLUSION

In the present paper we report three different Brillouin scattering experiments on molten $ZnCl_2$, which allow us to measure the relaxation times and elastic moduli for different geometries and polarizations. In a previous study of $ZnCl_2$ by depolarized light scattering [19], we showed that the relaxation function was well fitted by a single Cole-Davidson function added to an overdamped Lorentzian which took into account the high frequency part (i.e., above 100 GHz) of the spectrum and we were able to obtain from these experiments the relaxation times and stretching parameter of this Cole-Davidson function between 400 and 650 °C. In the present paper we show that introducing a simple Cole-Davidson function with the same stretching parameter, to describe the temperature dependent relaxation processes which couple to the longitudinal and transverse acoustic phonons, is sufficient to interpret our spectra. One test of our analysis is the determination of the static viscosity: shear viscosity values deduced from our measurements are in good agreement with direct measurements. This agrement is much poorer when the Cole-Davidson function is reduced to a Debye function. Similarly, using a Cole-Davidson function yields longitudinal, transverse, and rotational times proportional in the whole temperature range. This proportionality is not recovered in the case of a simple Debye process.

ACKNOWLEDGMENTS

One of us (M.J.L.) has benefited from a research grant from St-Gobain Recherches. We gratefully acknowledge NATO Cooperative Research Grant No. CRG-939730 which allowed a fruitful collaboration between University P. et M. Curie and New York City College. We also thank J. P. François for his help in the sample preparation and N. Fourcauld and N. Leprovost for their participation in some parts of the experiments.

[1] F. Mezei, W. Knaak, and B. Farago, Phys. Rev. Lett. **58**, 571 (1987); W. Petry, E. Bartsch, F. Fujara, M. Kiebel, H. Sillescu, and B. Farago, Z. Phys. B: Condens. Matter **83**, 175 (1991).

[2] G. Li, W. M. Du, A. Sakai, and H. Z. Cummins, Phys. Rev. A **46**, 3348 (1992).

[3] M. T. Cicerone and M. D. Ediger, J. Chem. Phys. **103**, 5684 (1995); R. Böhmer, G. Hinze, G. Diezemann, B. Geil, and H. Sillescu, Europhys. Lett. **36**, 55 (1996).

[4] W. Götze and L. Sjögren, Rep. Prog. Phys. **55**, 241 (1992); U. Bengtzelius, W. Götze, and A. Sjölander, J. Phys. C **17**, 5915 (1984); E. Leutheusser, Phys. Rev. A **29**, 2765 (1984); W. Götze, in *Liquids Freezing and the Glass Transition*, edited by J. P. Hansen, D. Levesque, and J. Zinn-Justin (North-Holland, Amsterdam, 1990), p. 287; S. P. Das and G. F. Mazenko, Phys. Rev. A **34**, 2265 (1986).

[5] H. Sillescu, J. Phys.: Condens. Matter **11**, A271 (1999); B. Doling and A. Heuer, *ibid.* **11**, A277 (1999); L. F. Cugliandolo and J. L. Iguain (unpublished).

[6] J. P. Hansen and I. R. Mc Donald, *Theory of Simple Liquids* (Academic, London, 1986); B. Berne and R. Pecora, *Dynamic Light Scattering* (Wiley, New York, 1976); J. P. Boon and S. Yip, *Molecular Hydrodynamics* (McGraw-Hill, New York, 1980).

[7] G. Li, W. M. Du, J. Hernandez, and H. Z. Cummins, Phys. Rev. E **48**, 1192 (1993).

[8] G. Li, W. M. Du, A. Sakai, and H. Z. Cummins, Phys. Rev. A **46**, 3343 (1992).

[9] (a) J. D. Mackenzie and W. K. Murphy, J. Chem. Phys. **33**, 366 (1960); (b) A. J. Easteal and C. A. Angell, *ibid.* **56**, 4231 (1972).

[10] G. S. Gruber and T. A. Litovitz, J. Chem. Phys. **40**, 13 (1964).

[11] R. Triolo and A. H. Narten, J. Chem. Phys. **74**, 703 (1981); J. A. Erwin Desa, A. C. Wright, J. Long, and R. N. Sinclair, J. Non-Cryst. Solids **51**, 57 (1982).

[12] S. Biggin and J. E. Enderby, J. Phys. C **14**, 3129 (1981); D. A. Allen, R. A. Howe, N. D. Wood, and W. S. Howells, J. Chem. Phys. **94**, 5071 (1991); E. Kartini, M. F. Collins, F. Mezei, and E. C. Svensson, Physica B **234-236**, 399 (1997).

[13] F. Aliotta, G. Maisano, P. Migliardo, C. Vasi, F. Wanderlingh, G. Pedro-Smith, and R. Triolo, J. Chem. Phys. **75**, 613 (1981); F. Aliotta, M. P. Fontana, G. Maisano, P. Migliardo, C. Vasi, and F. Wanderlingh, J. Phys. Colloq. C6 **42**, 57 (1981).

[14] H. E. G. Knape, J. Chem. Phys. **80**, 4788 (1984).

[15] H. Zhu, Y. Sato, T. Yamamura, and K. Sugimoto, Ber. Bunsenges. Phys. Chem. **97**, 583 (1993).

[16] M. Soltwitsch, J. Sukmanowski, and D. Quitmann, J. Chem. Phys. **86**, 3207 (1987).
[17] S. N. Yannopoulos and E. A. Pavlatou, Proceedings of the Eighth International Symposium on Molten Salts, edited by R. J. Gale, G. Blomgrem, and H. Kojima [**16**, 258 (1992)].
[18] M. Grimsditch and N. Rivier, Appl. Phys. Lett. **58**, 2345 (1991).
[19] M. J. Lebon, C. Dreyfus, G. Li, A. Aouadi, H. Z. Cummins, and R. M. Pick, Phys. Rev. E **51**, 4537 (1995).
[20] E. A. Pavlatou, S. N. Yannopoulos, G. N. Papatheodorou, and G. Fytas, J. Phys. Chem. **101**, 8748 (1997).
[21] M. Wilson and P. A. Madden, J. Phys.: Condens. Matter **5**, 6833 (1993); M. C. C. Ribeiro, M. Wilson, and P. A. Madden, J. Chem. Phys. **108**, 9027 (1998); **110**, 4803 (1999).
[22] (a) G. P. Johari and M. Goldstein, J. Chem. Phys. **55**, 4245 (1971); (b) E. Rössler, Phys. Rev. Lett. **69**, 1620 (1992); D. Richter, R. Zorn, B. Farago, B. Frick, and L. J. Fetters, *ibid.* **69**, 1621 (1992).
[23] R. D. Mountain, J. Res. Natl. Bur. Stand., Sect. A **70**, 207 (1966); R. D. Mountain, Rev. Mod. Phys. **38**, 205 (1966).
[24] H. C. Andersen and R. Pecora, J. Chem. Phys. **54**, 2584 (1971); **55**, 1496 (1971); P. J. Chapell, M. P. Allen, P. I. Hallen, and D. Kivelson, *ibid.* **74**, 5929 (1981), and references therein.
[25] C. Dreyfus, A. Aouadi, R. M. Pick, T. Berger, A. Patkowski, and W. Steffen, Europhys. Lett. **42**, 55 (1998); Eur. Phys. J. B **9**, 401 (1999).
[26] C. H. Wang, Mol. Phys. **58**, 497 (1986).
[27] B. Quentrec, Phys. Rev. A **15**, 1304 (1977).
[28] J. C. Maxwell, Philos. Trans. R. Soc. London **49**, 157 (1867).
[29] W. M. Du, G. Li, H. Z. Cummins, M. Fuchs, J. Toulouse, and L. A. Knauss, Phys. Rev. E **49**, 2192 (1994).
[30] C. P. Lindsey and G. D. Patterson, J. Chem. Phys. **73**, 3348 (1980).
[31] S. M. Lindsay, M. W. Anderson, and J. R. Sandercock, Rev. Sci. Instrum. **52**, 1478 (1981); G. Li, N. Tao, L. V. Hong, H. Z. Cummins, C. Dreyfus, M. Hebbache, R. M. Pick, and J. Vagner, Phys. Rev. B **42**, 440 (1990).
[32] M. Grimsditsch, R. Bhadra, and L. M. Torell, Phys. Rev. Lett. **62**, 2616 (1989).
[33] C. Dreyfus, M. J. Lebon, H. Z. Cummins, J. Toulouse, B. Bonello, and R. M. Pick, Phys. Rev. Lett. **69**, 3666 (1992).
[34] T. A. Litovitz and C. M. Davis, *Physical Acoustics*, edited by W. P. Mason (Academic, New-York, 1965), Vol. 2, p. 281.